

Analyzing Numerical Errors in Domain Heat Transport Models Using the CVBEM

T. V. Hromadka II

Hydrologist,
U.S. Geological Survey,
Laguna Niguel, Calif. 92677

Besides providing an exact solution for steady-state heat conduction processes (Laplace-Poisson equations), the CVBEM (complex variable boundary element method) can be used for the numerical error analysis of domain model solutions. For problems where soil-water phase change latent heat effects dominate the thermal regime, heat transport can be approximately modeled as a time-stepped steady-state condition in the thawed and frozen regions, respectively. The CVBEM provides an exact solution of the two-dimensional steady-state heat transport problem, and also provides the error in matching the prescribed boundary conditions by the development of a modeling error distribution or an approximate boundary generation. Consequently, this error evaluation can be used to develop highly accurate CVBEM models of the heat transport process, and the resulting model can be used as a test case for evaluating the precision of domain models based on finite elements or finite differences.

Introduction

In previous papers, Hromadka and Guymon [1] applied the complex variable boundary element method (CVBEM) to the problem of predicting freezing fronts in two-dimensional soil systems. It is noted that although the CVBEM moving boundary phase change model of Hromadka and Guymon [1] will determine the steady-state location of the freezing front, the modeling process must evolve through a time history of the freezing front movement from a prescribed initial location. Hromadka et al. [2] subsequently compare the CVBEM solution to a domain solution method and prototype data for the Deadhorse Airport runway at Prudhoe Bay, Alaska. An example in using domain methods to model a moving interface in heat transfer problems is given in Yoo and Rubinsky [3]. In another work, the model is further extended to include an approximation of soil water flow (Hromadka and Guymon [4]).

An example in the use of real variable boundary element methods (Brebbia [5]) for moving boundary phase change problems and a review of the literature is given in O'Neill [6].

Hromadka and Guymon [7] develop a relative error estimation scheme which exactly evaluates the relative error distribution on the problem boundary that results from the CVBEM approximation matching the known boundary conditions. This relative error determination is used to add or delete boundary nodes to improve accuracy. Thus, the CVBEM permits a direct and immediate determination of the approximation error involved in solution of an assumed Laplacian system. The modeling accuracy is evaluated by the model-user in the determination of an approximative boundary upon which the CVBEM provides an exact solution.

Although inhomogeneity (and anisotropy) can be included in the CVBEM model, the resulting fully populated matrix system quickly becomes large. Therefore in this paper, the domain is assumed homogeneous and isotropic except for differences in frozen and thawed conduction parameters on either side of the freezing front.

In this paper, the main effort is to present a procedure for evaluating the accuracy of the domain models of soil-water phase change. The two types of error evaluated are equation (1) errors in heat flux estimation due to domain model discretization, and equation (2) phase change moving boundary approximative error. The CVBEM (see Appendix A) is used to provide the quasi-analytic solution to the boundary problem for comparison with the domain model. Use of the "approximative boundary" technique for evaluating the CVBEM error, and hence developing highly accurate CVBEM models, is presented in Appendix B. After the analyst is satisfied that the domain model is adequate, inhomogeneity can be introduced or long-term simulations initiated.

Domain Model Discretization Evaluation

A popular method for approximating heat flow effects is by means of numerical modeling. Generally domain methods are used, such as finite elements and finite difference, although collocation methods and boundary integral equations methods have also been employed. In the domain methods the problem domain is discretized by nodal points into control volumes or finite elements. The choice as to nodal point placement is usually based on the judgment and experience of the analyst. Generally, the nodal point density is increased in regions where the state variable (e.g., temperature) is anticipated to vary rapidly with respect to either space or time. Additional placement of nodal points is governed by the

Contributed by the OMAE Division for publication in the JOURNAL OF OFFSHORE MECHANICS AND ARCTIC ENGINEERING. Manuscript received by the OMAE Division October 24, 1986.

interface between dissimilar materials or boundary condition specifications.

In this section, the main objective is to present a technique for identifying regions within the problem domain where the nodal point density needs to be increased to reduce error in modeling heat flux over nodal point control volumes. The basis of the procedure is to examine the accuracy of the numerical model in predicting steady-state conditions where various boundary conditions are considered. In order to examine the steady-state predicted values, the Complex Variable Boundary Element Method or CVBEM is used to develop nodal point approximation values and estimates of nodal point modeling error. Nodal points are then added (or removed when possible) in regions where the domain model estimates of the steady-state values differ significantly from the CVBEM predicted values. In this fashion, the conduction process modeling error due to choice of discretization is reduced.

Two-dimensional models of heat transport have been extensively reported in the literature. Generally, either a finite element or finite difference method is used to develop a system of algebraic equations of nodal point values as functions of the problem domain, heat parameters, and boundary conditions. For example,

$$\frac{\partial}{\partial x} \left(K_x \frac{\partial \phi}{\partial x} \right) + \frac{\partial}{\partial y} \left(K_y \frac{\partial \phi}{\partial y} \right) = C \frac{\partial \phi}{\partial t} \quad (1)$$

where

ϕ = temperature
 K_x, K_y = x and y -direction thermal conductivities
 C = heat capacity

For homogeneous, isotropic domains equation (1) can be rewritten as

$$\frac{\partial^2 \phi}{\partial x^2} + \frac{\partial^2 \phi}{\partial y^2} = \frac{C}{K} \frac{\partial \phi}{\partial t} \quad (2)$$

Application of a domain numerical method results in a matrix system

$$[K]\phi + [C]\dot{\phi} = F \quad (3)$$

where $[K]$ is a symmetrical banded matrix representing the heat flow rates from the nodal point control volumes; $[C]$ is a symmetric banded matrix representing the capacitance of the nodal point control volumes; F is a vector of specified nodal point values and flux boundary conditions (with $[K]$ and $[C]$ appropriately modified); and ϕ and $\dot{\phi}$ are the vectors of nodal point values and their time derivatives. Hromadka et al. [2] show that an infinity of domain methods can be described by equation (3) when written in form

$$[K] + [C(\eta)]\dot{\phi} = F \quad (4)$$

where $\eta = 2, \infty, \dots$ results in the Galerkin finite element formulation, subdomain integration, and an integrated finite difference formulation, respectively.

In this paper, only errors in approximating the heat flux are considered. To evaluate the numerical errors resulting from the $[K]$ matrix, a steady-state problem is solved of the form

$$[K]\phi = \hat{F} \quad (5)$$

where \hat{F} is a vector representing the boundary conditions for a selected steady-state scenario. Usually, several boundary value problems are considered resulting in several approximations in the form of equation (5) which can be examined for numerical error development. However, to evaluate the error in equation (5), the ϕ vector needs to be compared to the correct solution vector ϕ^* . Because an analytic solution

for equation (5) is seldom available, the CVBEM is used to develop another approximation vector ϕ' and a corresponding relative error distribution. The ϕ' values represent a highly accurate estimate of the exact solution values ϕ^* , such that $|\phi^* - \phi'|$ is small. The ϕ' vector is then used for comparison purposes with the domain model solution of ϕ in order to locate regions where the domain method approximation deviates substantially from the CVBEM approximation values.

Moving Boundary Error Evaluation

For steady-state conditions, the governing heat flow equations reduce to the Laplace equation (the transient heat capacitance term is omitted). The following assumptions are utilized (Fig. 1):

- 1 The two-dimensional soil system is rigid with negligible deformations due to frost heave. (Deformations could easily be included in a general purpose model by including an appropriate frost heave approximation procedure.)
- 2 The soil system is completely frozen above the freezing point and completely thawed below the freezing point.
- 3 The soil-water flow is assumed negligible.
- 4 All boundary conditions are assumed constant for all time.
- 5 The soil system is homogeneous and isotropic (or the system is rescaled such that the modified domain is homogeneous and isotropic).
- 6 The effects of ice-lensing at the freezing front are ignored.
- 7 The steady-state heat conduction processes are modeled by the two-dimensional Laplace equation.

The steady-state conditions are evaluated by solving simultaneously

$$\begin{aligned} K_f \nabla^2 \phi_f &= 0, \quad \text{in } \Omega_f \text{ (frozen)} \\ K_t \nabla^2 \phi_t &= 0, \quad \text{in } \Omega_t \text{ (thawed)} \end{aligned} \quad (6)$$

where ϕ is the potential temperature function and (K_f, K_t) are the frozen and thawed thermal conductivities corresponding to the respective domains (Ω_f, Ω_t). On the freezing front (assumed 0°-C isotherm) the conditions required are

$$\phi_f = \phi_t = 0, \quad (x, y) \in C \quad (7)$$

and

$$K_f \frac{d\phi_f}{dS} = -K_t \frac{d\phi_t}{dS} \quad (8)$$

where (ϕ_f, ϕ_t) are the frozen and thawed temperatures on the freezing front contour, C ; and ψ is the stream function which is conjugate to the potential ϕ ; and S is a tangential coordinate on C .

The procedure starts by developing a CVBEM approximator $\hat{\omega}_f(z)$ and $\hat{\omega}_t(z)$ for the frozen and thawed domains, respectively. Hromadka and Guyman [8] gives the details for developing such CVBEM approximators. The numerical technique determines the analytic function $\hat{\omega}(z)$, which satisfies

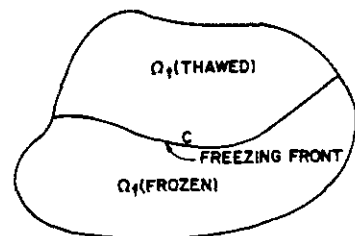


Fig. 1 Problem definition

the boundary conditions of either normal flux or temperature specified at nodal points located on the problem boundary, Γ . Because $\omega(z)$ is analytic throughout the interior domain Ω , which is enclosed by Γ , then the real and imaginary parts of $\omega(z) = \phi(z) + i\psi(z)$ both exactly satisfy the Laplace equation over Ω . (This property afforded by the CVBEM is not guaranteed by any of the domain methods, such as finite elements or finite differences.)

For the steady-state condition, the governing heat flow equations reduce to the Laplace equations shown in equation (6). Consequently, a $\omega(z)$ determined for both the frozen and thawed regions satisfy the Laplace equations exactly, leaving only errors in satisfying the boundary conditions. To develop a CVBEM steady-state solution, a $\omega(z)$ is developed for each of the separate regions. Initially, both $\omega_f(z)$ and $\omega_r(z)$ are defined by (Fig. 1)

$$\begin{aligned} \omega_f(z) &= \omega_f^1, \quad z \in \Omega_f \\ \omega_r(z) &= \omega_r^1, \quad z \in \Omega_r \end{aligned} \quad (9)$$

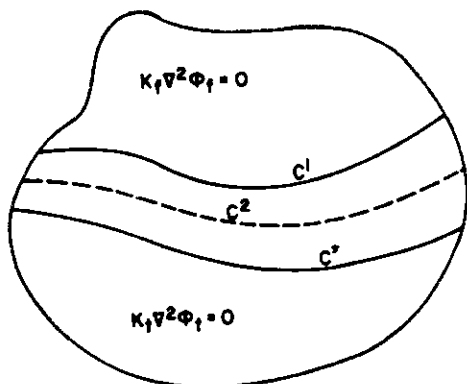


Fig. 2 Redefining the freezing front location

where in equation (9) $\Omega = \Omega_f \cup \Omega_r$ is the global domain, and the first-order CVBEM approximators are based on the entire domain. This procedure results in simply estimating the 0°-C isotherm location for the homogeneous problem of Ω being entirely frozen or thawed. Let C^1 be the contour corresponding to this 0°-C isotherm.

The second iteration step begins by defining Ω_f^2 and Ω_r^2 and Ω_f^2 and Ω_r^2 , respectively.

Examining the stream functions ψ_f^2 and ψ_r^2 , estimates of the discrepancy in meeting equation (8) are evaluated. The ω_f^2 function is now used to determine the next location of the 0°-C isotherm. This is accomplished by determining a new ω_f^* (and modified by conductivity) superimposed at the nodal values of C^1 . Next, a new 0°-C isotherm is located for ω_f^* . The next estimated location for the 0°-C isotherm, C^2 , is located by averaging the y -coordinates of the nodal points between C^1 and C^* . Figure 2 illustrates this procedure.

The third iteration step proceeds by defining Ω_f^3 and Ω_r^3 based on the mutual boundary of C^2 and the foregoing procedure is repeated.

The iteration process continues until the final estimates of Ω_f and Ω_r are determined with corresponding ω_f and ω_r approximators, such that

$$|K_f d\hat{\psi}_f/ds - K_r d\hat{\psi}_r/ds| < \epsilon, \quad z \in C \quad (10)$$

Applications

Figure 3 depicts an application of the geothermal model for a roadway embankment problem and the use of the approximative boundary. Figure 4 illustrates the two-dimensional steady-state freezing front location for a geothermal problem involving a buried subfreezing 3-m-dia pipeline. An examination of the approximative boundaries indicate that a good CVBEM approximator was determined by use of a 26-node CVBEM model. The maximum departure δ between the approximative boundaries and the problem boundary Γ occurred along the top of the pipeline and had a value of

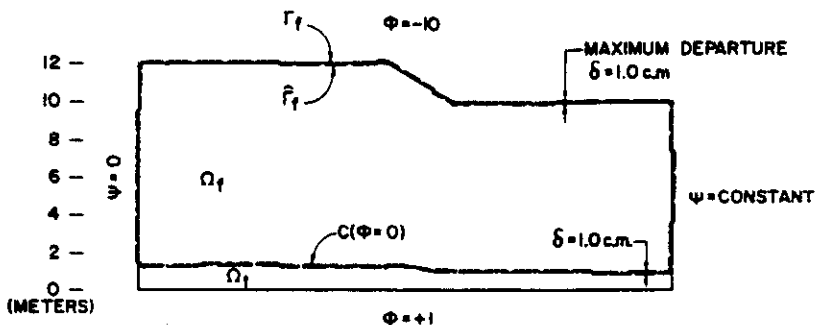


Fig. 3 The approximative boundary $\hat{\Gamma}$, and the goodness-of-fit to the problem boundary, Γ

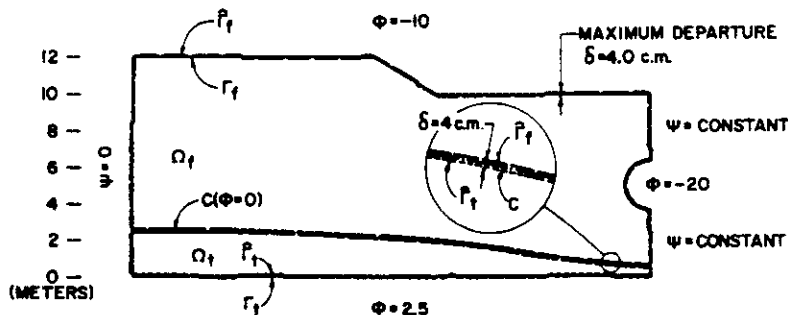


Fig. 4 Application of the CVBEM geothermal model to predict steady-state conditions

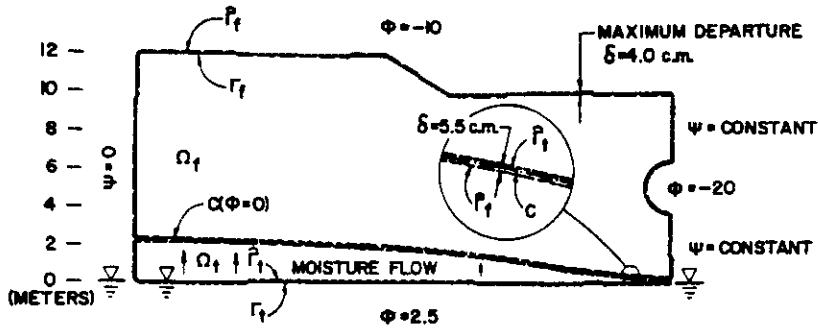


Fig. 5 Application of the CVBEM coupled model

approximately 3.5 cm. The average departure $\bar{\delta}$ is estimated at less than 1 cm.

The freezing front maximum departure is approximately 4 cm and occurred at the right-hand side. Average departure on C is less than 2 cm. By the Maximum Modulus theorem, the error $|\phi^* - \phi'|$ must have a maximum on the boundary; thus interior of the domain model errors are bounded accordingly.

Conclusions

From the figures it is seen that the CVBEM approximations are good estimates for the freezing front location. This evaluation is based upon the close fit between the problem and the CVBEM approximative boundary. That is, if the approximative boundary is assumed to be the constructed version of the problem, then the CVBEM is the exact solution to the steady-state boundary value problem.

Thus, the CVBEM can be used to develop a quasi-analytic solution to the boundary problems which occur in freezing/thawing studies. The CVBEM model is then used to compare with domain solutions in order to evaluate the numerical error.

After a satisfactory performance of the domain model is obtained, various parameter values (e.g., nonhomogeneity) can be introduced and long-term simulations initiated.

References

- 1 Hromadka II, T. V., and Guymon, G. L., "Application of a Boundary Integral Equation to Prediction of Freezing Fronts in Soils," *CRST*, Vol. 6, 1981, pp. 115-121.
- 2 Hromadka II, T. V., Guymon, G. L., and Berg, R. L., "Comparison of Two-Dimensional Domain and Boundary Integral Geothermal Models with Embankment Freeze-Thaw Field Data," *Permafrost*, Fourth International Conference, Proceedings, National Academy Press, 1983.
- 3 Yoo, J., and Rubinsky, B., "Numerical Computation Using Finite Elements for the Moving Interface in Heat Transfer Problems with Phase Transformation," *Numerical Heat Transfer*, Vol. 6, 1983.
- 4 Hromadka II, T. V., and Guymon, G. L., "Simple Model of Ice Segregation Using an Analytic Function to Model Heat and Soil Water Flow," Third International Symposium on Offshore Mechanics and Arctic Engineering, New Orleans, La.; also, *ASME Journal of Energy Resources Technology*, Sept. 1984.
- 5 Brebbia, C. A., *The Boundary Element Method for Engineers*, Pentech Press, 1980.
- 6 O'Niell, K., "Boundary Integral Equation Solution of Moving Boundary Phase Change Problems," *International Journal of Numerical Methods Engineering*, Vol. 19, 1983, pp. 1825-1850.
- 7 Hromadka II, T. V., and Guymon, G. L., "An Algorithm to Reduce Approximation Error from the CVBEM," *Numerical Heat Transfer*, 1984.
- 8 Hromadka II, T. V., and Guymon, G. L., "The Complex Variable Boundary Element Method: Development," *International Journal of Numerical Methods in Engineering*, 1984.
- 9 Hromadka II, T. V., *The Complex Variable Boundary Element Method*, Springer-Verlag, 1984.

APPENDIX A:

Complex Variable Boundary Element Method

Hromadka and Guymon [8] present a detailed development of the CVBEM. A comprehensive presentation of the method is given in Hromadka [9]. A feature available with the CVBEM is the generation of a relative error measure which can be used to match the known boundary condition values of the problem. Consequently, the method can be used to develop a highly accurate approximation function for the Laplace equation and yet provide a descriptive relative error distribution for analysis purposes. Because the main objective of this paper is to analyze the numerical error in solving equation (5), it is noted that the Laplace equation is solved throughout the problem domain (if homogeneous) or in connected subregions (if nonhomogeneous). Many anisotropic effects can be accommodated by the usual rescaling procedures or by subdividing the total domain into easier-to-handle

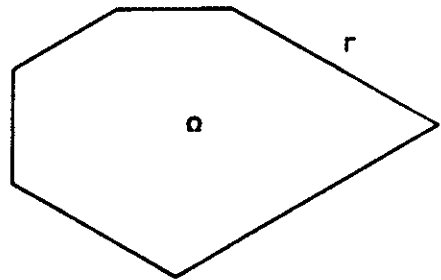


Fig. 6 Simply connected domain Ω with simple closed contour boundary Γ

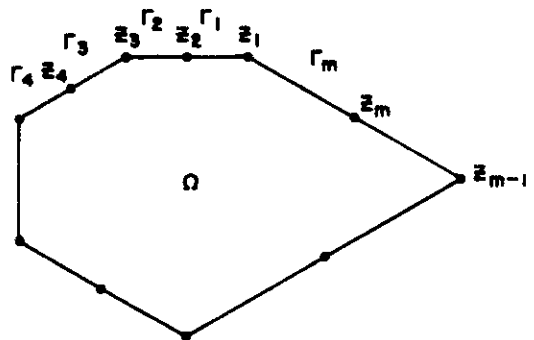


Fig. 7 Γ discretized into m boundary elements

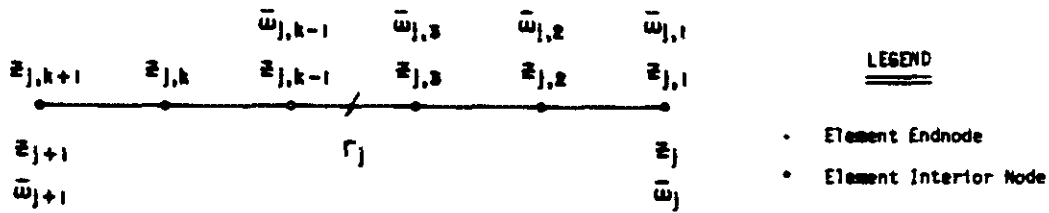


Fig. 8 $(k + 1)$ -node boundary element Γ_j nodal definitions

subproblems. The CVBEM is then applied to the problem domain(s) as discussed in the following.

Let Ω be a simply connected domain with boundary Γ where Γ is a simple closed contour (Fig. 6). Discretize Γ by m nodal points into m boundary elements such that a node is placed at every angle point on Γ (Fig. 7). Each boundary element is defined by

$$\Gamma_j = \{z: z = z(s)\}$$

where

$$z(s) = z_j + (z_{j+1} - z_j)s, \quad 0 \leq s \leq 1, \quad j \neq m \quad (11)$$

with the exception that on the last element

$$\Gamma_m = \{z: z = z(s)\}$$

where

$$z(s) = z_m + (z_1 - z_m)s, \quad 0 \leq s \leq 1$$

Then

$$\Gamma = \bigcup_{j=1}^m \Gamma_j \quad (12)$$

Let each Γ_j be discretized by $(k + 1)$ evenly spaced nodes ($k \geq 1$) such that Γ_j is subdivided into k equal length segments (Fig. 8). The Γ_j is said to be a $(k + 1)$ -node element. From Fig. 8, each Γ_j has an associated nodal coordinate system such that $z_{j,1} = z_j$ and $z_{j,k+1} = z_{j+1} = z_{j+1,1}$.

On each Γ_j , define a local coordinate system by

$$\begin{aligned} \zeta_j(s) &= z_{j,1} + (z_{j,k+1} - z_{j,1})s, \quad 0 \leq s \leq 1 \\ &= z_j + (z_{j+1} - z_j)s \end{aligned} \quad (13)$$

where $d\zeta_j = (z_{j,k+1} - z_{j,1}) ds$.

On each $(k + 1)$ -node element Γ_j , a set of order k polynomial basis functions are uniquely defined by

$$N_{j,i}^k(s) = a_{j,i,0} + a_{j,i,1}s + \dots + a_{j,i,k}s^k \quad (14)$$

where $i = 1, 2, \dots, (k + 1)$ and $0 \leq s \leq 1$, and where

$$N_{j,i}^k \left(\frac{z_{j,n} - z_{j,1}}{z_{j,k+1} - z_{j,1}} \right) = \begin{cases} 1, & n = i \\ 0, & n \neq i \end{cases} \quad (15)$$

The basis functions are further defined to have the property that for $\zeta \in \Gamma$

$$N_{j,i}^k \left(\frac{\zeta - z_{j,1}}{z_{j,k+1} - z_{j,1}} \right) = \begin{cases} N_{j,i}^k \left(\frac{\zeta - z_{j,1}}{z_{j,k+1} - z_{j,1}} \right), & \zeta \in \Gamma_j \\ 0, & \zeta \notin \Gamma_j \end{cases} \quad (16)$$

Let $\omega(z)$ be analytic on $\Omega \cup \Gamma$. That is, let $\omega(z)$ be the solution (unknown to the steady-state boundary condition problem being considered). At each nodal point on Γ , define a specified nodal value by (Fig. 8)

$$\bar{\omega}_{j,i} = \omega(z_{j,i}) \quad (17)$$

where from Fig. 8, $\bar{\omega}_{j,1} = \bar{\omega}_j = \bar{\omega}_{j-1,k+1}$. Using equation (16) and equation (17), an order k global trial function is defined

by

$$G^k(\zeta) = \sum_j G^k(\zeta_j(s)) = \sum_j \sum_{i=1}^k \bar{\omega}_{j,i} N_{j,i}^k \left(\frac{\zeta - z_{j,1}}{z_{j,k+1} - z_{j,1}} \right) \quad (18)$$

From equation (18), the global trial function is continuous on Γ . An H_k approximation function $\hat{\omega}_k(z)$ Hromadka [9] is defined by the Cauchy integral

$$\hat{\omega}_k(z) = \frac{1}{2\pi i} \int_{\Gamma} \frac{G^k(\zeta) d\zeta}{\zeta - z}, \quad z \in \Omega, \quad z \notin \Gamma \quad (19)$$

Because the derivative of $\hat{\omega}_k(z)$ exists for all $z \in \Omega$, then $\hat{\omega}_k(z)$ is analytic in Ω and exactly solves the Laplace equation in Ω .

Expanding equation (19) and using equation (12) gives

$$\int_{\Gamma} \frac{G^k(\zeta) d\zeta}{\zeta - z} = \sum_{j=1}^m \int_{\Gamma_j} \frac{G^k(\zeta) d\zeta}{\zeta - z} \quad (20)$$

Integrating on boundary element j gives (Hromadka [9])

$$\begin{aligned} \int_{\Gamma_j} \frac{G^k(\zeta) d\zeta}{\zeta - z} &= R_j^{k-1}(z) \\ &+ \sum_{i=1}^k \bar{\omega}_{j,i} N_{j,i}^k(\gamma_j) \ln \left(\frac{z - z_{j+1}}{z - z_j} \right) \end{aligned} \quad (21)$$

where $R_j^{k-1}(z)$ is an order $(k - 1)$ complex polynomial resulting from the circuit around point z (see Fig. 9) and γ_j is equal to $(z - z_j)/(z_{j+1} - z_j)$. Thus, the CVBEM results in the approximation function

$$\hat{\omega}_k(z) = \frac{1}{2\pi i} \sum_j \left(R_j^{k-1}(z) + \sum_i \bar{\omega}_{j,i} N_{j,i}^k(\gamma_j) \ln \left(\frac{z - z_{j+1}}{z - z_j} \right) \right) \quad (22)$$

or in a simpler form (Hromadka [9])

$$\hat{\omega}_k(z) = R^k(z) + \frac{1}{2\pi i} \sum_j \ln(z - z_j) \sum_i T_i^k \quad (23)$$

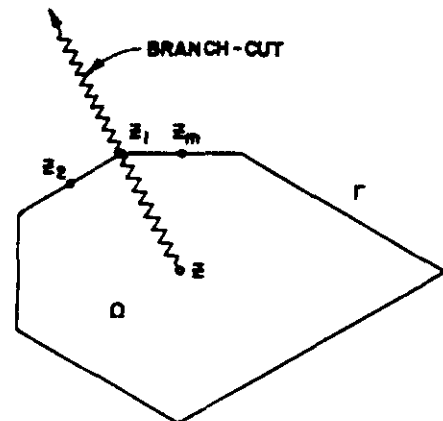


Fig. 9 Branch-cut of $\ln(z - \zeta)$ function, $\zeta \in \Gamma$

where $T_j^k = \bar{\omega}_{j-1,1} N_{j-1,1}^k(\gamma_{j-1}) - \bar{\omega}_{j,1} N_{j,1}^k(\gamma_j)$, and $R^k(z)$ follows from equation (22).

The approximation function of equation (23) exactly satisfies the governing flow equation in the problem domain Ω for the approximated boundary conditions on the problem boundary, Γ . Because $\bar{\omega}_k(z)$ is analytic on Ω , then the maximum relative error of $|\omega(z) - \bar{\omega}_k(z)|$ must occur on Γ . Consequently, the total approximation error can be simply evaluated on Γ with the corresponding errors on the interior of Ω being less in magnitude. Because the boundary conditions used to evaluate equation (23) are known continuously on Γ , then $\bar{\omega}_k(z)$ can be determined within arbitrary accuracy by the addition of nodal points on Γ due to (without proof)

$$2\pi i \lim_{\max|\Gamma_j| \rightarrow 0} \bar{\omega}_k(z) = \int_{\Gamma} \frac{\lim_{\max|\Gamma_j| \rightarrow 0} G^k(\xi) d\xi}{\xi - z} = \int_{\Gamma} \frac{\omega(\xi) d\xi}{\xi - z} = 2\pi i \omega(z) \quad (24)$$

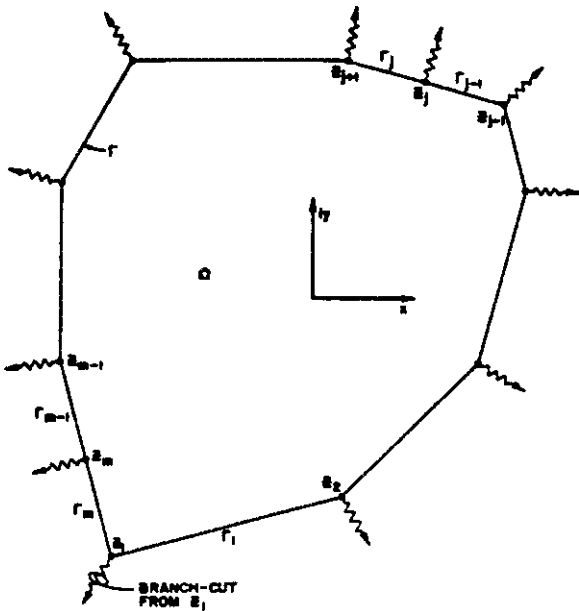
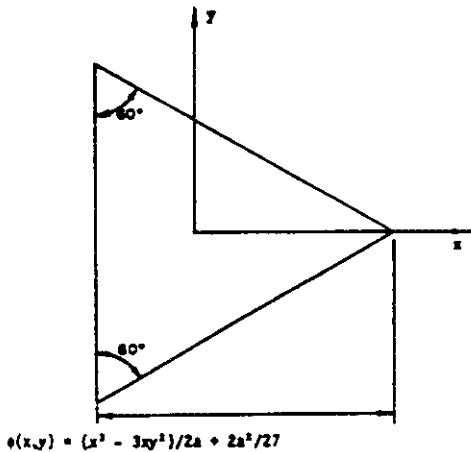


Fig. 10 The analytic continuation of $\bar{\omega}(z)$ to the exterior of $\Omega \cup \Gamma$. Note branch cuts along Γ at nodes z_j .



$$\phi(x, y) = (x^2 - 3xy^2)/2a + 2a^2/27$$

Fig. 11 Application problem geometrics and exact solutions for temperature, $\phi(x, y)$

APPENDIX B:

The Approximative Boundary for CVBEM Error Analysis

Generally, the prescribed boundary conditions are values of constant ϕ or ψ on each Γ_j . These values correspond to level curves of the analytic function $\omega(z) = \phi + i\psi$. After determining a $\bar{\omega}(z)$, it is convenient to determine an approximate boundary $\bar{\Gamma}$ which corresponds to the level curves of $\bar{\omega}(z) = \bar{\phi} + i\bar{\psi}$ which are specified as the prescribed boundary conditions. The resulting contour $\bar{\Gamma}$ is a visual representation of approximation error, and $\bar{\Gamma}$ coincident with Γ implies that $\bar{\omega}(z) = \omega(z)$. Additional collocation points are located at regions where $\bar{\Gamma}$ deviates substantially from Γ .

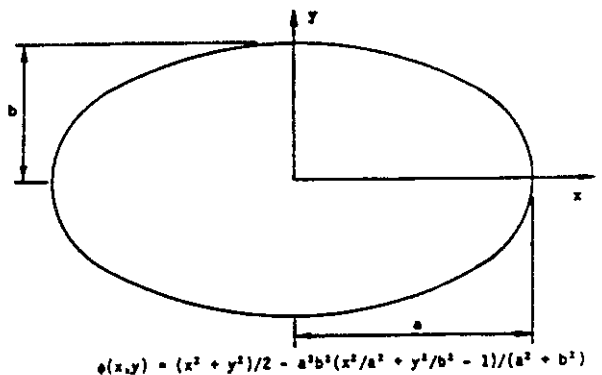
A difficulty in using this method of locating collocation points is that the contour $\bar{\Gamma}$ cannot be determined for points z outside of $\Omega \cup \Gamma$. To proceed, an analytic continuation of $\bar{\omega}(z)$ to the exterior is achieved by rewriting the integral function equation (9) in terms of

$$\frac{1}{2\pi i} \int_{\Gamma} \frac{G(\xi) d\xi}{\xi - z} = R_1(z) + \sum_{j=1}^m (\alpha_j + i\beta_j)(z - z_j) \text{Ln}(z - z_j) \quad (25)$$

where α_j and β_j are real numbers; and $\text{Ln}(z - z_j)$ is a principal value logarithm with branch-cuts drawn normal to Γ from each branch point z_j , such as shown in Fig. 10. The resulting approximation is analytic everywhere except on each branch-cut. The $R_1(z)$ function in equation (25) is a first-order reference polynomial which results due to the integration circuit of 2π radians along Γ . If $\omega(z)$ is not a first-order polynomial, then $R_1(z)$ can be omitted in equation (10).

Implementation on a computer is direct, although considerable computation effort is required. One strategy for using this technique is to subdivide each Γ_j with several internal points (about 4 to 6) and determine $\bar{\omega}(z)$ at each point. Next, $\bar{\Gamma}$ is located by a Newton-Raphson stepping procedure in locating where $\bar{\omega}(z)$ matches the prescribed level curve. Thus, several evaluations of $\bar{\omega}(z)$ are needed to locate a single $\bar{\Gamma}$ point. The end product, however, may be considered very useful since it can be argued that $\bar{\omega}(z)$ is the exact solution to the boundary value problem with Γ transformed to $\bar{\Gamma}$, and $\bar{\Gamma}$ is a visual indication of approximation error.

The use of the method discussed for locating additional collocation points on Γ is demonstrated by application of the



$$\phi(x, y) = (x^2 + y^2)/2 - a^2 b^2 (x^2/a^2 + y^2/b^2 - 1)/(a^2 + b^2)$$

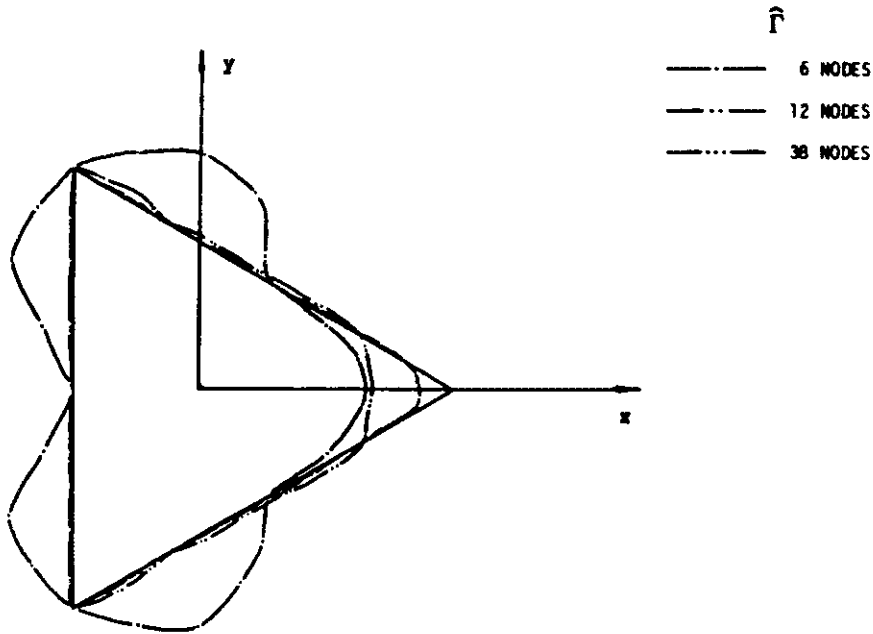


Fig. 12 Approximate boundaries for three nodal point distributions

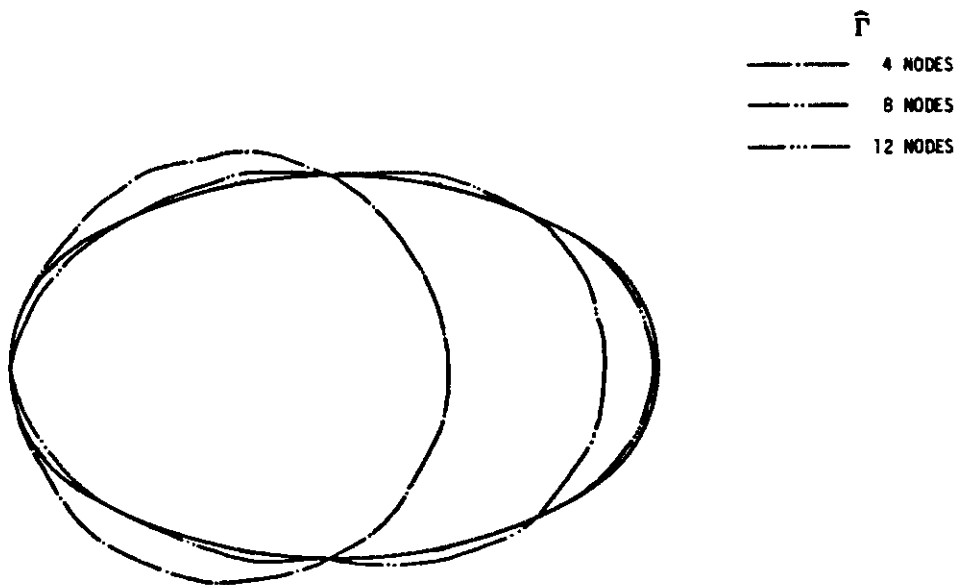


Fig. 13 Approximate boundaries for three nodal point distributions

CVBEM for solving 2 steady-state heat transfer problems. The problems considered each involve a different geometry and set of boundary conditions of the Dirichlet class. The analytic solution to the problems are included in Fig. 11. Each solution satisfies the Laplace equation and is defined as a function of a local coordinate $x - y$ system with an origin specified as shown in the figures. On the problem boundaries, Γ , the potential function or temperature is also a continuous function of position defined by

$$\phi(z \in \Gamma) = \frac{1}{2}(x^2 + y^2) \quad (26)$$

From equation (26), it is seen that the boundary conditions are not level curves; consequently, the determination of an approximative boundary $\hat{\Gamma}$ requires further definition. In

these applications, the problem is approached by using the statement

$$\hat{\Gamma} \equiv \{z: \hat{\phi}(z) = \frac{1}{2}(x^2 + y^2) = \frac{1}{2}|z|^2\} \quad (27)$$

The strategy of working with level curves (i.e., $\phi = \phi_j$ for $z \in \Gamma_j, j = 1, 2, \dots, m$), follows analogously.

The two applications illustrate the development of CVBEM approximation functions which exactly satisfy the governing partial differential equation (Laplace equation) in Ω and approximately satisfy the boundary conditions which are continuously specified on Γ . The subsequent figures illustrate the CVBEM error evaluations along Γ for evenly spaced nodal placements for each problem boundary.